Springer
the language of science

Dear Dr/Prof. Andrey Grachev,

Here are the electronic proofs of your article.

- You can submit your corrections **online** or by **fax**. Together with your proof corrections you must return the *Copyright Transfer Statement* to complete the proof process.
- **Print out** the *proof*. (If you do not already have Acrobat Reader, just download it from http://www.adobe.com.)
- Check the metadata sheet to make sure that the header information, especially author names and the corresponding affiliations are correctly shown.
- Check that the text is complete and that all figures, tables and their legends are included. Also check the accuracy of special characters, equations, and electronic supplementary material if applicable. If necessary refer to the *Edited manuscript*.
- The publication of inaccurate data such as dosages and units can have serious consequences. Please take particular care that all such details are correct.
- Please **do not** make changes that involve only matters of style. We have generally introduced forms that follow the journal's style. Substantial changes in content, e.g., new results, corrected values, title and authorship are not allowed without the approval of the responsible editor. In such a case, please contact the Editorial Office and return his/her consent together with the proof.
- For **online** submission please insert your corrections in the online correction form [available in your eProof webpage]. Always indicate the line number to which the correction refers.
- For **fax** submission, please ensure that your corrections are clearly legible. Use a fine black pen and write the correction in the margin, not too close to the edge of the page.
- The cover sheets (including the *Copyright Transfer Statement* and the *Offprint Order Form*) can either be scanned and sent electronically or sent by fax.
- If we do not receive your corrections within 48 hours, we will send you a reminder.

Please note

This is the **official first publication** citable with the DOI. **Further changes are, therefore, not possible**.

After online publication, subscribers (personal/institutional) to this journal will have access to the complete article via the DOI using the URL: http://dx.doi.org/[DOI].

If you would like to know when your article has been published online, take advantage of our free alert service. For registration and further information go to: http://www.springerlink.com.

Due to the electronic nature of the procedure, the manuscript and the original figures will only be returned to you on special request. When you return your corrections, please inform us if you would like to have these documents returned.

The **printed version** will follow in a forthcoming issue.

Springer
the language of science

Andrey Grachev
NOAA Earth System Research Laboratory
Boulder, CO, : Exp , USA
Email: Andrey.Grachev@noaa.gov

OFFPRINT ORDER
AID: 9177
MS Ref No.:
DOI: 10.1007/s10546-007-9177-6

Re: **Sheba flux profile relationships in the stable atmospheric boundary layer**

By: **Andrey Grachev · Edgar Andreas · Christopher Fairall · Peter Guest · P. Persson**

To be published in: **Boundary-Layer Meteorology**

Dear Andrey Grachev,

This is to let you know that the above publication has gone into production and will appear in due course. Offprints of your article may be ordered by filling out and returning this form.

I would like to receive:

50 offprints free of charge

_____________ additional offprints without cover (minimum of 50 offprints)

Orders for offprints are only accepted if received with payment or if accompanied by an official purchase order from your institution, failing which no offprints can be produced. Postage and handling cost are absorbed by the publishers. Payment can be made by credit card, bankdraft personal check or international money order. UNESCO coupons are also accepted. Payment is accepted in any hard currency. Prices of additional offprints and delivery terms are mentioned on the enclosed price list.
Make checks payable to Springer Science + Business Media – Dordrecht

☐ I enclose payment to the amount of __________________________

☐ Please charge my credit card account

Card no.: ______________________________ Expiry date: ________________________

☐ Access ☐ Eurocard ☐ American Express ☐ Bank Americard

☐ Visa ☐ Diners club ☐ Master Card

I enclose official purchase order no.: __________________________

VAT identification no.: ____

Date ______________________________ Signature _______________________________

PLEASE CHECK YOUR ADDRESS AND CORRECT IF NECESSARY

TERMS OF DELIVERY

1. A minimum of 50 offprints may be ordered. Prices corresponding to the number of pages and quantities ordered are given below.

2. Author for correspondence will receive this offprint order form. This author is therefore also responsible for any orders the co-authors wish to make. All orders for a particular paper should appear together on only one form.

3. Offprints are printed at the same time the book or journal is printed. Thus, no alterations from the exact form in which the article appears in a book or journal are possible. Any orders for offprints that are received after the book or journal is printed should be submitted to the Production Secretariat at the address below.

4. Offprints will be forwarded within a short time after the appearance of the published paper.

5. No additional offprints can be printed or sent unless this order form is filled in, signed, returned with appropriate payment or official purchase order and received before the book or journal goes to press.

6. Any correspondence in connection with offprints must state the name of the periodical, title and offprint order number and name(s) of the author(s). In case of camera-ready publications please inform us as soon as possible, preferably by fax, about the number of offprints you wish to order.
All communications should be sent to Springer, Manufacturing Department, P.O. Box 990, 3300 AZ, Dordrecht / Van Godewijckstraat 30, 3311 GX Dordrecht, The Netherlands.
ABN-AMRO Bank, Dordrecht 50.80.13.917, Postal Cheque Account Number 4447384.

Prices of additional offprints are in EUR

Number of copies	Number of pages					
	1-4	5-8	9-12	13-16	17-20	+4
50	108	177	248	318	388	71
100	153	238	323	407	492	85
150	200	300	400	500	599	100
200	246	361	476	591	706	115
250	292	422	551	681	810	130
300	339	483	628	772	917	145
350	385	544	703	863	1022	159
400	431	606	780	955	1129	175
450	478	667	857	1046	1235	189
500	524	728	932	1136	1340	204
+50	+50	+62	+72	+92	+103	+15

Payment will be accepted in any convertible currency. Please check the rate of exchange with your bank.
If ordering from within The Netherlands please add 19% VAT to the price quoted above.

As of January 1st 1993 customers within the EEC must consider the following rules:

- **If you are in possession of a VAT identification number, please fill the VAT number in on the order form. You will not be charged VAT.**
- **If you do *not* have a VAT number, then please add the low VAT rate - applicable to your country - to the prices quoted above.**

Fax to: +44 870 762 8807 (UK) or +91 44 4208 9499 (INDIA)

Springer

From: **Springer Correction Team**
6&7, 5th Street, Radhakrishnan Salai, Chennai, Tamil Nadu, India – 600 004

Re: **Boundary-Layer Meteorology DOI: 10.1007/s10546-007-9177-6**
Sheba flux profile relationships in the stable atmospheric boundary layer

Authors: **Andrey Grachev · Edgar Andreas · Christopher Fairall · Peter Guest · P. Persson**

I. Permission to publish

I have checked the proofs of my article and

- ❑ I have **no corrections.** The article is ready to be published without changes.
- ❑ I have **a few corrections.** I am enclosing the following pages:
- ❑ I have made **many corrections.** Enclosed is the **complete article.**

Date / signature ____

II. Copyright Transfer Statement (sign only if not submitted previously)

The copyright to this article is transferred to Springer Science+Business Media, B.V. (for government employees: to the extent transferable) effective if and when the article is accepted for publication. The author warrants that his/her contribution is original and that he/she has full power to make this grant. The author signs for and accepts responsibility for releasing this material on behalf of any and all co-authors. The copyright transfer covers the exclusive right to reproduce and distribute the article, including reprints, translations, photographic reproductions, microform, electronic form (offline, online) or any other reproductions of similar nature.

An author may self-archive an author-created version of his/her article on his/her own website and his/her institution's repository, including his/her final version; however he/she may not use the publisher's PDF version which is posted on www.springerlink.com. Furthermore, the author may only post his/her version provided acknowledgement is given to the original source of publication and a link is inserted to the published article on Springer's website. The link must be accompanied by the following text: "The original publication is available at www.springerlink.com."

The author is requested to use the appropriate DOI for the article (go to the Linking Options in the article, then to OpenURL and use the link with the DOI). Articles disseminated via www.springerlink.com are indexed, abstracted and referenced by many abstracting and information services, bibliographic networks, subscription agencies, library networks, and consortia.

After submission of this agreement signed by the corresponding author, changes of authorship or in the order of the authors listed will not be accepted by Springer.

Date / Author's signature ____

Springer
the language of science

ELECTRONIC REPRINT ORDER FORM

After publication of your journal article, electronic (PDF) reprints may be purchased by arrangement with Springer and Aries Systems Corporation.

The PDF file you will receive will be protected with a copyright system called DocuRights®. Purchasing 50 reprints will enable you to redistribute the PDF file to up to 50 computers. You may distribute your allotted number of PDFs as you wish; for example, you may send it out via e-mail or post it to your website. You will be able to print five (5) copies of your article from each one of the PDF reprints.

Please type or print carefully. Fill out each item completely.

1. Your name: ______________________________

   Your e-mail address: ______________________________

   Your phone number: ______________________________

   Your fax number: ______________________________

2. Journal title (vol, iss, pp): ______________________________

3. Article title: ______________________________

4. Article author(s): ______________________________

5. How many PDF reprints do you want? ______________________________

6. Please refer to the pricing chart below to calculate the cost of your order.

Number of PDF reprints	Cost (in U.S. dollars)
50	$200
100	$275
150	$325
200	$350

NOTE: Prices shown apply only to orders submitted by individual article authors or editors. Commercial orders must be directed to the Publisher.

All orders must be prepaid. Payments must be made in one of the following forms:

- a check drawn on a U.S. bank
- an international money order
- Visa, MasterCard, or American Express (no other credit cards can be accepted)

PAYMENT (type or print carefully):

Amount of check enclosed: ________________ (payable to Aries Systems Corporation)

VISA ______________________________

MasterCard ______________________________

American Express ______________________________

Expiration date: ________________ Signature: ______________________________

Print and send this form with payment information to:

Aries Systems Corporation
200 Sutton Street
North Andover, Massachusetts 01845
Attn.: Electronic Reprints
— OR —
Fax this to Aries at: 978-975-3811

Your PDF reprint file will be sent to the above e-mail address. If you have any questions about your order, or if you need technical support, please contact: support@docurights.com

Springer
the language of science

Proof correction marks to be used by authors

Marginal mark	Meaning	Corresponding mark in text	
	Delete (take out)	/ or ⊢⊣	Cross through
	Delete and close-up		Above and below matter to be taken out
stet	Leave as printed (when matter has been crossed out by mistake)	------	Under matter to remain
caps	Change to capital letters	≡	Under letters or words altered
l.c.	Change to lower case letters		Encircle letters altered
bold	Change to bold type	~~~	Under matter altered
bold ital.	Change to bold italic type		Under matter altered
ital.	Change to italics	———	Under matter altered
rom.	Change to roman type		Encircle matter altered
X	Replace by similar but undamaged character or remove extraneous marks		Encircle letter to be altered
	Insert (or substitute) superior figure or sign	⋏ or /	
	Insert (or substitute) inferior figure or sign	⋏ or /	
	Insert (or substitute) hyphen	⋏ or /	
EN	Insert (or substitute) dash	⋏ or /	
(/)	Insert (or substitute) solidus	⋏ or /	
•••	Insert (or substitute) ellipsis	⋏ or /	
	Close-up - delete space		Linking words or letters
#	Insert space	| or Y	Between items
equal #	Make spacing equal	|	Between items
↑	Reduce space	| or ↑	Between items
≻—	Insert space between lines or paragraphs		
←	Reduce space between lines or paragraphs		
	Transpose		Between letters or words, numbered when necessary
	Transpose lines		
centre	Place in centre of line	] [	Around matter to be centered
	Move to the left		
	Move to the right		
NP	Begin a new paragraph	□	Before first word of new paragraph
run on	No fresh paragraph here		Between paragraphs
⋏	(Caret mark.) Insert matter indicated in margin	⋏	
	Insert single / double quotes	⋏⋏	

Remarks

To indicate a substitution, simply cross out the letters or words to be replaced, and write the correct letters or words in the margin. It is not necessary, nor even desirable, to use the marks for *delete* and *insert* when making a substitution. If there is more than one substitution in a line, place them in the correct order in the margin, and indicate the end of each correction with an oblique stroke / . Alternatively, continental location marks may be used, but these are to be placed in front of the corrections, not behind as in the case of the oblique stroke.
The typesetter treats *all* letters and words in the margin as insertions or substitutions, so - to avoid misunderstanding - any comments *not* intended to form part of the text should be encircled.
All alterations should be marked clearly so that there is no risk of misunderstanding; long additions or amendments should be typed on separate slips and attached. *Only really essential alterations should be made at proof stage.*
In addition to reading the proofs, please look through your edited manuscript to see if there are *any queries from the copy editor,* and if so, answer the queries *on the proofs.*

Springer
the language of science

COLOUR CONSENT FORM

Dear Andrey Grachev,

Springer offers two options for reproducing colour illustrations in our publications. Check the author instructions for the submission of electronic figures.
Please select the option you prefer:

Option 1 ☐	***Free Online Colour***	Colour figures will only appear in colour on www.springerlink.com **and not** in the printed version of the journal
Option 2 ☐	***Online and Printed Colour***	Colour figures will appear in colour on www.springerlink.com **and** in the printed version of the journal

Charges Springer charges authors for the reproduction of colour figures in print.
The charges are **€ 950** or **$ 1150** per article. If you agree to the colour charges then please complete the form below:

Journal Title (abbreviated title):	Boundary-Layer Meteorology
Manuscript Number:	9177
Article Title:	Sheba flux profile relationships in the stable atmospheric ...
Author's name:	Andrey Grachev
Invoice Address:	NOAA Earth System Research Laboratory Boulder, CO, : Exp , USA

I enclose payment to the amount of **€ 950 / $ 1150**

Please charge my credit card account (incl. check digits): ____ ____ ____ ____ ___

Expiry date: __ __ – __ __

☐ Access ☐ Visa ☐ Eurocard ☐ American Express ☐ Bank Americard ☐ Diners Club ☐ Master Card

Date

Signature

Regardless whether you have chosen option 1 or 2, please sign and return this form.

HOW TO USE THE CORRECTION GRID

[1] Put the page number of each correction in the Page Number column.

[2] Put the line numbers of each correction in the Line Number column.

[3] Write the number of the equation, table or figure that needs correction in the Equation Number, Table Number or Figure Number columns.

[4] Insert the text/symbols you wish to be changed in the Incorrect column.

[5] Insert the correct text/symbols in the Correct column. If you include extra text/symbols here, indicate the exact items that need to be changed by highlighting them in the color red (for example 'The outer membrane surface…' corrected to 'The outer membrane surface…').

[6] Our typesetter queries on the galley proof regarding insufficient information or required clarifications will already be inserted into the grid (in the Page Number, Line Number and Incorrect columns). Please answer these queries by putting the relevant information in the Correct column. If you are unable to answer a query, indicate this by putting the letters 'NA' in the Correct column.

[7] New versions of figures/tables can be included as an 'attachment' to the Correction Grid e-mail.

[8] If you need to add more rows to the grid, press the TAB key on your keyboard when you are in the last row.

[9] The Correction Grid is a basic Microsoft Word table. If you do not use Microsoft Word, please return corrections in RTF format similar to the example provided below.

Example of how to use the correction grid

MANUSCRIPT I.D.: ABCD 1234

Page Number	**Line Number**	**Equation Number**	**Table Number**	**Figure Number**	**Incorrect**	**Correct**	**Not for Author use**
1	16				Sith	Smith	
5			3		Caption: Amount of CO inhalation person	Caption: Amount of CO inhalation per person	
7				4	Replace figure with new one on attachment to this e-mail		
10		19			X (X-1)	X (Y-1)	

CORRECTION GRID

MANUSCRIPT I.D.:

Page Number	Line Number	Equation Number	Table Number	Figure Number	Incorrect	Correct	Not for Author use

Metadata of the article that will be visualized in OnlineFirst

ArticleTitle	Sheba flux–profile relationships in the stable atmospheric boundary layer	
Article Sub-Title		
Journal Name	Boundary-Layer Meteorology	
Corresponding Author	Family Name	**Grachev**
	Particle	
	Given Name	**Andrey A.**
	Suffix	
	Division	Cooperative Institute for Research in Environmental Sciences
	Organization	University of Colorado
	Address	Boulder, CO, USA
	Division	
	Organization	NOAA Earth System Research Laboratory
	Address	Boulder, CO, USA
	Email	Andrey.Grachev@noaa.gov
Author	Family Name	**Andreas**
	Particle	
	Given Name	**Edgar L.**
	Suffix	
	Division	
	Organization	U.S. Army Cold Regions Research and Engineering Laboratory
	Address	Hanover, NH, USA
	Division	
	Organization	NorthWest Research Associates, Inc. (Bellevue Division)
	Address	25 Eagle Ridge, 03766-1900, Lebanon, NH, USA
	Email	
Author	Family Name	**Fairall**
	Particle	
	Given Name	**Christopher W.**
	Suffix	
	Division	
	Organization	NOAA Earth System Research Laboratory
	Address	Boulder, CO, USA
	Email	
Author	Family Name	**Guest**
	Particle	
	Given Name	**Peter S.**
	Suffix	
	Division	
	Organization	Naval Postgraduate School
	Address	Monterey, CA, USA
	Email	

Author	Family Name	**Persson**
	Particle	
	Given Name	**P. Ola G.**
	Suffix	
	Division	Cooperative Institute for Research in Environmental Sciences
	Organization	University of Colorado
	Address	Boulder, CO, USA
	Division	
	Organization	NOAA Earth System Research Laboratory
	Address	Boulder, CO, USA
	Email	

	Received	6 March 2006
Schedule	Revised	
	Accepted	2 March 2007

Abstract

Measurements of atmospheric turbulence made during the Surface Heat Budget of the Arctic Ocean Experiment (SHEBA) are used to examine the profile stability functions of momentum, ϕ_m, and sensible heat, ϕ_h, in the stably stratified boundary layer over the Arctic pack ice. Turbulent fluxes and mean meteorological data that cover different surface conditions and a wide range of stability conditions were continuously measured and reported hourly at five levels on a 20-m main tower for 11 months. The comprehensive dataset collected during SHEBA allows studying ϕ_m and ϕ_h in detail and includes ample data for the very stable case. New parameterizations for $\phi_m(\zeta)$ and $\phi_h(\zeta)$ in stable conditions are proposed to describe the SHEBA data; these cover the entire range of the stability parameter $\zeta = z/L$ from neutral to very stable conditions, where L is the Obukhov length and z is the measurement height. In the limit of very strong stability, ϕ_m follows a $\zeta^{1/3}$ dependence, whereas ϕ_h initially increases with increasing ζ, reaches a maximum at $\zeta \approx 10$, and then tends to level off with increasing ζ. The effects of self-correlation, which occur in plots of ϕ_m and ϕ_h versus ζ, are reduced by using an independent bin-averaging method instead of conventional averaging.

Keywords (separated by '-'): Arctic Ocean - Flux–profile relationships - Monin–Obukhov similarity theory - SHEBA Experiment - Stable boundary layer

Footnote Information

Boundary-Layer Meteorol
DOI 10.1007/s10546-007-9177-6

ORIGINAL PAPER

Sheba flux–profile relationships in the stable atmospheric boundary layer

Andrey A. Grachev · Edgar L. Andreas · Christopher W. Fairall · Peter S. Guest · P. Ola G. Persson

Received: 6 March 2006 / Accepted: 2 March 2007

Abstract Measurements of atmospheric turbulence made during the Surface Heat Budget of the Arctic Ocean Experiment (SHEBA) are used to examine the profile stability functions of momentum, φ_m, and sensible heat, φ_h, in the stably stratified boundary layer over the Arctic pack ice. Turbulent fluxes and mean meteorological data that cover different surface conditions and a wide range of stability conditions were continuously measured and reported hourly at five levels on a 20-m main tower for 11 months. The comprehensive dataset collected during SHEBA allows studying φ_m and φ_h in detail and includes ample data for the very stable case. New parameterizations for $\varphi_m(\zeta)$ and $\varphi_h(\zeta)$ in stable conditions are proposed to describe the SHEBA data; these cover the entire range of the stability parameter $\zeta = z/L$ from neutral to very stable conditions, where L is the Obukhov length and z is the measurement height. In the limit of very strong stability, φ_m follows a $\zeta^{1/3}$ dependence, whereas φ_h initially increases with increasing ζ, reaches a maximum at $\zeta \approx 10$, and then tends to

A. A. Grachev · P. O. G. Persson
Cooperative Institute for Research in Environmental Sciences,
University of Colorado, Boulder, CO, USA

A. A. Grachev (✉) · C. W. Fairall · P. O. G. Persson
NOAA Earth System Research Laboratory,
Boulder, CO, USA
e-mail: Andrey.Grachev@noaa.gov

E. L. Andreas
U.S. Army Cold Regions Research and Engineering Laboratory,
Hanover, NH, USA

Present address:
E. L. Andreas
NorthWest Research Associates, Inc. (Bellevue Division),
25 Eagle Ridge, Lebanon, NH 03766-1900, USA

P. S. Guest
Naval Postgraduate School,
Monterey, CA, USA

Journal: BOUN MS: BOUN77R2 CMS: 10546_2007_9177_Article ☐ TYPESET ☐ DISK ☐ LE ☐ CP Disp.:2007/3/14 Pages:

level off with increasing ζ. The effects of self-correlation, which occur in plots of φ_m and φ_h versus ζ, are reduced by using an independent bin-averaging method instead of conventional averaging.

Keywords Arctic Ocean · Flux–profile relationships · Monin–Obukhov similarity theory · SHEBA Experiment · Stable boundary layer

1 Introduction

Understanding the characteristics of turbulent transport to and from the Earth's surface is a central problem of atmospheric boundary-layer research. Traditionally, turbulent fluxes are derived from vertical wind speed and temperature profiles (flux–profile relationships), and the importance of the flux–profile relationships for climate modelling, weather forecasting, environmental impact studies, and many other applications has long been recognized.

Well-known predictions of the flux–profile relationships are based on the theory suggested over 50 years ago by Monin and Obukhov (1954). There is a long history of testing Monin–Obukhov predictions including profile functions (see, for example, the surveys in Monin and Yaglom 1971; Dyer 1974; Yaglom 1977; Dyer and Bradley 1982; Högström 1988; Sorbjan 1989; Garratt 1992; Andreas 2002). Perhaps the Businger–Dyer profile functions are the most widely and routinely used flux–profile relationships in the unstable case (Dyer and Hicks 1970; Paulson 1970; Businger et al. 1971). Considerably fewer studies exist that cover very stable conditions. In fact, a simple linear interpolation (log-linear law) proposed at the end of the 1960s by Zilitinkevich and Chalikov (1968) and Webb (1970) that provides blending between neutral and very stable cases is still widely used. Subsequently, several alternative empirical forms have been proposed for more strongly stable conditions (Holtslag and De Bruin 1988; Beljaars and Holtslag 1991).

Investigating the turbulence structure in the SBL is of great practical importance, especially for air pollution studies (Mahrt 1999), because the SBL develops almost every night over land surfaces. Progress in understanding the stable boundary layer (SBL) has been restrained because the SBL is often continually evolving and the turbulence is generally weak. In addition, several scaling regimes are identified in the SBL that are associated with different physical mechanisms (e.g., Holtslag and Nieuwstadt 1986; Smedman 1988; Mahrt et al. 1998; Grachev et al. 2005). Furthermore, several different definitions are possible for the SBL height (e.g., Zilitinkevich and Mironov 1996; Zilitinkevich and Baklanov 2002). Examining the SBL is also complicated by slope flows, low-level jets, meandering motions, influence of gravity waves, and other phenomena (e.g., Mahrt 1999). Some insight into the SBL structure has been gained through several experimental studies (e.g., Forrer and Rotach 1997; Mahrt et al. 1998; Howell and Sun 1999; Pahlow et al. 2001; Yagüe et al. 2001; Mahrt and Vickers 2002; Klipp and Mahrt 2004; Cheng and Brutsaert 2005; Hartogensis and De Bruin 2005; Yagüe et al. 2006).

In this paper, we use the extensive dataset from the Surface Heat Budget of the Arctic Ocean Experiment (SHEBA) to study the profile stability functions and to derive new parameterizations for them in stable conditions. The SHEBA measurement program, which took place from October 1997 to October 1998, was the most ambitious scientific effort ever attempted in the Arctic (Andreas et al. 1999; Persson

Journal: BOUN MS: BOUN77R2 CMS: 10546_2007_9177_Article TYPESET DISK LE CP Disp.:2007/3/14 Pages:

et al. 2002). Turbulent fluxes and mean meteorological data were continuously measured at five levels on a 20-m main tower, supported by comprehensive atmospheric, oceanographic, and ice/snow data (Uttal et al. 2002). The 11 months of measurements during SHEBA cover a wide range of stability conditions, from weakly unstable to very stable stratification, and allow us to study the physical nature of the SBL, including the very stable cases, in detail.

Limited observations still remain a problem for SBL model validation. However, the turbulence data collected over the Arctic pack ice during SHEBA offer several advantages for studying the structure of the SBL compared to traditional nocturnal boundary-layer measurements at mid-latitudes. The theme that the polar regions are ideal meteorological "laboratories" is a recurrent one in the literature (cf. Andreas et al. 2000). At high latitudes, especially during the polar night, the long-lived SBL can reach very stable and quasi-stationary states. Besides, the Arctic pack ice is a rather uniform, flat surface without large-scale slopes, and as a result, our SHEBA data are not contaminated by drainage (katabatic) or strong advective flows. The almost unlimited and extremely uniform fetch provides an opportunity to isolate many physical processes, with conditions that are nearly ideal for studying flux–profile relationships under stable conditions.

2 Formal background

Monin–Obukhov similarity theory (MOST) has provided a framework for describing turbulence in the stratified atmospheric surface layer. According to MOST (Monin and Obukhov 1954), properly scaled dimensionless statistics of the turbulence are universal functions of a stability parameter, $\zeta = z/L$, defined as the ratio of the reference height z and the Obukhov length scale (Obukhov 1946, 1971),

$$L = -\frac{u_*^3\,\theta_v}{\kappa g < w'\theta_v' >}, \tag{1}$$

where u_* is the friction velocity, θ_v is the virtual potential temperature, κ is the von Kármán constant, and g is the acceleration due to gravity. It should be noted that Eq. 1 is based on the *surface* momentum flux, $\tau_o = \rho u_*^2 = -\rho < u'w' >$, and the *surface* buoyancy flux, $b_o = (g/\theta_v) < w'\theta_v' >$ (ρ is air density, u and w are the longitudinal and vertical velocity components, respectively, $(')$ denotes fluctuations about the mean value, and $<\ \ >$ is a time/space averaging operator).

Specifically, the non-dimensional vertical gradients of mean wind speed (U) and potential temperature (θ) in the MOST are assumed to be

$$\frac{\kappa z}{u_*}\frac{\mathrm{d}U}{\mathrm{d}z} = \varphi_m(\zeta), \tag{2a}$$

$$\frac{\kappa z}{\theta_*}\frac{\mathrm{d}\theta}{\mathrm{d}z} = \varphi_h(\zeta), \tag{2b}$$

where $\theta_* = - < w'\theta' > /u_*$ is the temperature scale based on the *surface* potential temperature flux, and $\varphi_m(\zeta)$ and $\varphi_h(\zeta)$ are non-dimensional universal functions ('stability profile functions'). In this study, the traditional value of $\kappa = 0.4$ is used for both wind speed and temperature profiles.

The exact forms of the universal functions (2) are not predicted by MOST and must be determined from measurements. However, in the neutral case ($\zeta \equiv 0$) these functions equal unity by definition, and MOST does predict the asymptotic behaviour of these functions under very stable ($\zeta >> 1$) and extremely unstable stratification (free convection, $\zeta << -1$).

In the very stable case ($\zeta >> 1$), MOST predicts that specific quantities become independent of z; that is, z is no longer a primary scaling variable (Obukhov 1946; Monin and Obukhov 1954). This result is because stable stratification inhibits vertical motion, and the turbulence no longer communicates significantly with the surface (Monin and Yaglom 1971; Holtslag and Nieuwstadt 1986; Mahrt 1999). Wyngaard and Coté (1972) and Wyngaard (1973) apparently first referred to this limit as 'z-less stratification'. The z-less concept requires that z cancels in Eq. 2a,b, which leads to (e.g., Garratt 1992)

$$\varphi_m(\zeta) = \beta_m \zeta, \tag{3a}$$

$$\varphi_h(\zeta) = \beta_h \zeta, \tag{3b}$$

where β_m and β_h are numerical coefficients. It is worth noting that the original MOST predicts that only β_m in Eq. 3a is a constant, whereas β_h in Eq. 3b may be a function of ζ (see the discussion in Monin and Yaglom 1971, Sect. 7.3). Since MOST does not specify β_h, a constant value was subsequently accepted for β_h (e.g., Garratt 1992).

For near-neutral conditions and moderate ranges of ζ, observations suggest (e.g. Zilitinkevich and Chalikov 1968; Webb 1970)

$$\varphi_m(\zeta) = 1 + \beta_m \zeta, \tag{4a}$$

$$\varphi_h(\zeta) = 1 + \beta_h \zeta. \tag{4b}$$

with these linear equations fitting the available experimental data well for $\zeta < 1$ (Businger et al. 1971; Dyer 1974; Yaglom 1977; Dyer and Bradley 1982; Högström 1988; King 1990). Measurements suggest $\beta_m \approx \beta_h \approx 5$ (Sorbjan 1989; Garratt 1992). Note that Eq. 4a, b would be the linear approximation for fairly small values of ζ if Eq. 2a, b were expanded in a power series to yield (3a) and (3b) in the limit $\zeta \to \infty$.

During 1960–1980, the idea arose that Eq. 4 also applied for stronger stability, including the limit of very stable stratification (e.g., Garratt 1992). However, during the past decade, this view has been seriously challenged. Forrer and Rotach (1997), Howell and Sun (1999), Yagüe et al. (2001, 2006), Klipp and Mahrt (2004), and Cheng and Brutsaert (2005) reported that the stability functions increase more slowly with increasing stability than predicted by Eqs. 3 or 4; and moreover, one (φ_h) or both functions become approximately constant in very stable conditions. Based on an analysis of standard deviations covering almost five orders of magnitude in ζ, Pahlow et al. (2001) found that they do not follow the z-less predictions; their results, therefore, suggest that the concept of z-less stratification generally does not hold. In Sect. 4, we consider in detail the behaviour of the φ_m and φ_h functions in the limit of very strong stability based on the SHEBA data.

The wind speed and temperature profiles in the general, non-neutral case are derived by integrating Eq. 2a, b (Panofsky 1963). Traditionally, these integral forms of the flux–gradient relations are expressed with the neutral and diabatic contributions separated:

$$U(z) = \frac{u_*}{\kappa}\left[\ln\frac{z}{z_o} - \Psi_m\left(\frac{z}{L}\right) + \Psi_m\left(\frac{z_o}{L}\right)\right], \tag{5a}$$

$$\theta(z) - \theta_o = \frac{\theta_*}{\kappa}\left[\ln\frac{z}{z_{ot}} - \Psi_h\left(\frac{z}{L}\right) + \Psi_h\left(\frac{z_{ot}}{L}\right)\right]. \tag{5b}$$

Here, θ_o is the surface potential temperature, z_o is the aerodynamic roughness length, and z_{ot} is the temperature roughness length. The functions Ψ_m in Eq. 5a and Ψ_h in Eq. 5b obey

$$\Psi_m(\zeta) = \int_0^{\zeta} \frac{1-\varphi_m(\xi)}{\xi}\mathrm{d}\xi, \tag{6a}$$

$$\Psi_h(\zeta) = \int_0^{\zeta} \frac{1-\varphi_h(\xi)}{\xi}\mathrm{d}\xi. \tag{6b}$$

The purpose of our study is to revisit the empirical functional forms of φ_m, φ_h, Ψ_m, and Ψ_h for stable conditions based on the SHEBA data.

3 The SHEBA dataset

The SHEBA ice camp was centred around the Canadian icebreaker *Des Groseilliers*, which was frozen into the Arctic ice pack and drifted in the Beaufort Gyre from early October 1997 until early October 1998. During this period, the icebreaker drifted more than 2800 km in the Beaufort and Chukchi seas, with coordinates varying from approximately 74° N and 144° W to 81° N and 166° W.

Turbulent fluxes and mean meteorological data were continuously measured at five levels, nominally 2.2, 3.2, 5.1, 8.9, and 18.2 m (or 14 m during most of the winter), on the 20-m main SHEBA tower. Each level on the main tower had a Väisälä HMP-235 temperature and relative humidity probe and identical Applied Technologies, Inc. (ATI) three-axis sonic anemometer/thermometers (K-probe) that sampled at 10 Hz. An Ophir fast infrared hygrometer was mounted at about 8 m above the snow or ice surface (just below level 4). Except for rare periods, instruments ran almost continuously during 11 months. Turbulent covariance values and appropriate variances at each level are based on 1-h averaging and derived through the frequency integration of the cospectra and spectra (for other details, see in Persson et al. (2002)).

Several data-quality indicators based on objective and subjective methods have been applied to the original flux data. Flux data have been edited for unfavourable relative wind direction for which the tower and the other camp structures were upwind of the sonic anemometers, noting that the wind blew from disturbed areas only about 10% of the time. Most of the station structures and the *Des Groseilliers* itself were located within these sectors. The undisturbed sector at SHEBA had a natural sea ice surface for many hundreds of kilometres with almost unlimited and uniform fetch. Some other quality-control criteria are based on validity limits for the horizontal (σ_u and σ_v) and vertical (σ_w) velocity standard deviations: $\sigma_u < 2\,\mathrm{m\,s^{-1}}$, $\sigma_v < 2\,\mathrm{m\,s^{-1}}$, and $\sigma_w < 0.7\,\mathrm{m\,s^{-1}}$. The main SHEBA tower was instrumented for over 8000 h, with over 6000 h of that period yielding useful data.

A number of corrections traditionally are applied for eddy-covariance measurements, many of which result from limitations in the instruments or non-ideal boundary-layer conditions (i.e., advection, non-simple terrain). As mentioned earlier the Arctic pack ice is a rather uniform, flat surface without large-scale slopes and heterogeneity. For this reason, coordinate system rotation to account for the slope of the terrain (Wilczak et al. 2001) and corrections for advection (Paw U et al. 2000) are not required in our case.

Note that while Kaimal and Finnigan (1994, p. 219) suggested that ATI sonic anemometers not be used below a height of 4 m for adequate flux estimates, Kristensen and Fitzjarrald (1984) pointed out that adequate flux measurements can be made at heights of several (4–5) times the anemometer path separation. With a path length between transducers of 0.15 m, the ATI anemometer can be used for accurate variance measurements as low as 0.6 m. Andreas et al. (2006) showed that, because of path separation, flux measurements made by ATI sonic anemometers should be performed at least 1.7 m above the surface to avoid significant flux loss in SHEBA data. This result is a little stronger than Kristensen and Fitzjarrald (1984) estimations above. All measurements at SHEBA, including level 1 (2.2 m), satisfied these criteria.

In our analysis no corrections on the turbulent fluxes for loss of spectral energy (e.g., Moore 1986; Horst 2000; Massman 2000) were performed. Errors caused by inadequate frequency response and sensor separations depend on wind speed, boundary-layer stability, the height of the sensors above the ground, and the type of instruments deployed. However, they are insignificant for the sensible heat and momentum fluxes in our case (Andreas et al. 2006, pp. 123–124). Note also that according to Forrer and Rotach (1997), the corrections for the sensible heat flux and for friction velocity, which were measured with one single instrument (i.e., anemometer/thermometer), are typically less than 10% for $\zeta = 0.1$. These corrections on the latent heat flux (basically due to the sensor separation) may be 40% (their Fig. 4), but the moisture correction term in ζ and in sonic temperature is usually small for Arctic conditions (Grachev et al. 2005, p. 205).

Comprehensive analysis of different flux frequency response correction methods (Moore 1986: Horst 2000; Massman 2000; and their variations) was performed by Clement (2004). According to the Clement (2004) study, different methods for stable conditions give an average net correction between 1% and 2% for sensible heat flux (Ibid. Fig. 7.9) and less than 2% for the momentum flux (Ibid. Fig. 7.13). However, Clement (2004) also found that, for low wind speeds, flux loss for sensible heat flux can be up to 30% (Ibid. Fig. 7.11). Because low wind speeds are usually associated with strong stability, these corrections to the sensible heat flux at $\zeta = 100$ can be as large as 5–30% for different methods (Ibid. Fig. 7.12). The same conclusions can be applied to the momentum flux; large corrections are associated with low wind speeds (Ibid. Fig. 7.15) and very stable stratification (Ibid. Fig. 7.16). To avoid possible significant flux loss, wind speeds $\leq$ m s^{-1} have been excluded from our data. According to the Clement (2004) study, flux loss corrections for stable conditions are less than 5–10% (for the different methods tested) under this restriction (Ibid. Figs. 7.11 and 7.15).

The 'slow' temperature and humidity probes provided air temperature and relative-humidity measurements at five levels and were used to evaluate the vertical temperature gradient in Eq. 2. The mean wind speed was derived from the sonic anemometers. Rotation is needed to place the measured wind components in a streamwise coordinate system. We used the most common method, which is a double rotation of the anemometer coordinate system, to compute the longitudinal, lateral, and vertical velocity components.

The vertical gradients in Eq. 2 were obtained by fitting the following second-order polynomial through the 1-h profiles:

$$x(z) = p_1(\ln z)^2 + p_2 \ln z + p_3, \quad (7)$$

Journal: BOUN MS: BOUN77R2 CMS: 10546_2007_9177_Article TYPESET DISK LE CP Disp.:2007/3/14 Pages:

where $x(z)$ represents either the wind speed, U, or the potential temperature, θ, at measurement level z, and p_1, p_2, and p_3 are the polynomial coefficients. The gradients and, thus, φ_m and φ_h were determined by taking the derivative of Eq. 7 with respect to z and evaluating it at each of the five tower levels.

Other details of the SHEBA program, the ice camp, deployed instruments, data processing, accuracy, calibration, and archived data files can be found in Andreas et al. (1999, 2002, 2003, 2006), Persson et al. (2002), Uttal et al. (2002), and Grachev et al. (2002, 2005).

4 Profile functions observed during SHEBA

The comprehensive SHEBA dataset allows us to study in detail the behaviour of φ_m and φ_h and other relevant turbulent features under stable conditions and sheds light on their behaviour in the limit of very strong stability. In this section, we consider different aspects of how φ_m and φ_h depend on the bulk Richardson number and ζ, with special emphasis on spurious self-correlation.

Traditionally, the non-dimensional gradients φ_m and φ_h are plotted versus ζ. However, a troubling feature of this analysis is that the same variables (primarily u_*) appear in both the definitions of φ_m and φ_h and in ζ, see Eqs. 1 and 2. For this reason, analyses for φ_m and φ_h versus ζ may have built-in correlation (or self-correlation) that can lead to erroneous results (e.g., Hicks 1978; Mahrt et al. 1998; Andreas and Hicks 2002; Klipp and Mahrt 2004). For example, decreasing u_* increases ζ and φ_m and decreases φ_h. As a result, dependencies of φ_m and φ_h on ζ could be due to self-correlation, is also referred to as artificial, fictitious, or spurious correlation.

To obtain more reliable and independent estimates of the stability profile functions (2) over a wide range of stable conditions, we plot φ_m and φ_h versus the bulk Richardson number,

$$\mathrm{Ri}_B = -\left(\frac{gz}{\theta_v}\right)\frac{(\Delta\theta + 0.61\theta_v\Delta q)}{U^2}, \quad (8)$$

where $\Delta\theta$ and Δq are differences in the potential temperature and the specific humidity, respectively, between the surface and reference level z. Figures 1 and 2 show such plots for φ_m and φ_h for both surface and local scaling. Functions $\varphi_{m\,(1)}$ and $\varphi_{h\,(1)}$ in Figs. 1a and 2a are based on the fluxes measured at level 1 ('surface fluxes'), whereas $\varphi_{m\,(n)}$ and $\varphi_{h\,(n)}$ in Figs. 1b and 2b are based on the local fluxes at height z_n ($n = 1-5$) rather than on the surface values (Nieuwstadt 1984; Holtslag and Nieuwstadt 1986; Sorbjan 1989). Wind-speed and temperature gradients in these functions, $\varphi_{m\,(1)}$, $\varphi_{m\,(n)}$, $\varphi_{h\,(1)}$, and $\varphi_{h\,(n)}$, are referred to level n. The bin-averaged points in Figs. 1 and 2, based on the averaging of the individual one-hour data for Ri_B, φ_m, and φ_h are indicated by different symbols for each measurement level.

The individual 1-h-averaged data based on the median fluxes and other medians (heights, temperatures, etc.) for the five levels are also shown in Figs. 1 and 2 as background x-symbols. These points give an estimate of the available data at all levels and the typical scatter of the data. The median fluxes are computed from the median cospectra (i.e., at each frequency a median is computed from the values from the heights where data are available). The vertical dashed lines correspond to a critical Richardson number. According to the SHEBA data (Grachev et al. 2002, 2005), a

Journal: BOUN MS: BOUN77R2 CMS: 10546_2007_9177_Article TYPESET DISK LE CP Disp.:2007/3/14 Pages:

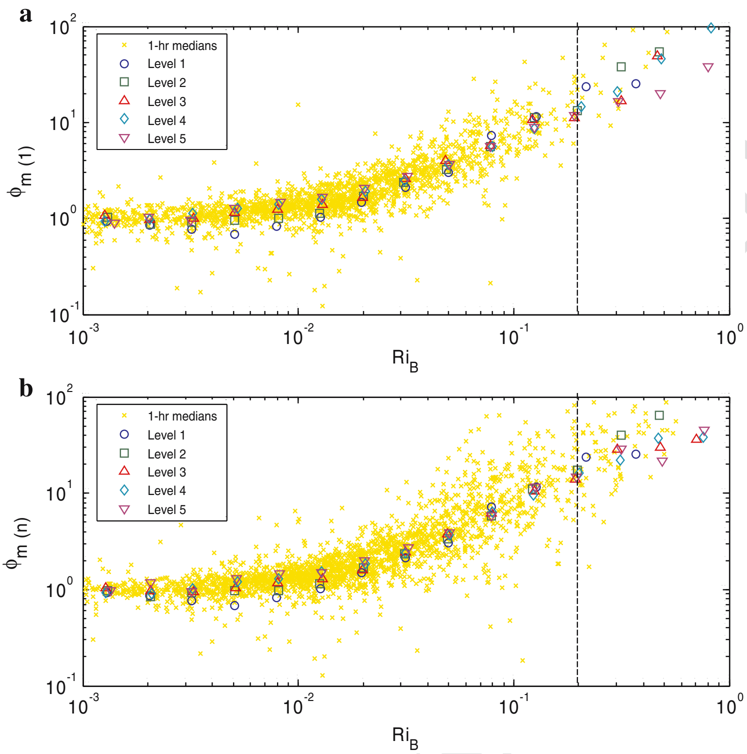

Fig. 1 Plots of the bin-averaged non-dimensional velocity gradient, φ_m, against the bulk Richardson number, Ri_B, for levels 1–5 during the 11 months of measurements. The functions φ_m in panel *a* are based on the fluxes measured at level 1 ('surface fluxes'), whereas φ_m in panel *b* are based on the local fluxes ($n = 1 - 5$). The vertical dashed lines correspond to $\mathrm{Ri}_B = 0.2$. Individual 1-h averaged data based on the median fluxes for the five levels are shown as the background x-symbols

bulk Richardson number, Eq. 8, of about 0.2 may be considered as the critical value; that is, $\mathrm{Ri}_{B\ cr} \approx 0.2$.

Figures 1 and 2 show that the averaged stability functions have different behaviours in the very stable regime. According to Fig. 1, φ_m increases with increasing stability up to the critical Richardson number. At the same time, φ_h, shown in Fig. 2, initially increases with increasing Ri_B and then almost levels off at $\mathrm{Ri}_B \approx 0.1$ (Fig. 2a). Figure 1 shows that there is no visible difference in plots for φ_m if we use surface (Fig. 1a) or local scaling (Fig. 1b). However, according to Fig. 2, using surface scaling instead of local scaling leads to less scatter between different observation levels for φ_h (cf. Grachev et al. 2005).

Although plots of φ_m and φ_h versus Ri_B are useful for qualitative analyses of these functions, theoretical formulations and parameterizations assume a functional dependence of φ_m and φ_h on ζ. Before plotting the φ_m and φ_h functions versus ζ, it is necessary to determine a range of ζ that corresponds to values $\mathrm{Ri}_B < 0.2$. Figure 3 shows ζ plotted against Ri_B for different levels. Although the dependence of ζ on Ri_B is not a universal function an average value of $\zeta = O(10)$ may be associated with $\mathrm{Ri}_B \approx 0.2$. However, some individual points in Fig. 3 for which $\mathrm{Ri}_B < 0.2$ reach values

Journal: BOUN MS: BOUN77R2 CMS: 10546_2007_9177_Article TYPESET DISK LE CP Disp.:2007/3/14 Pages:

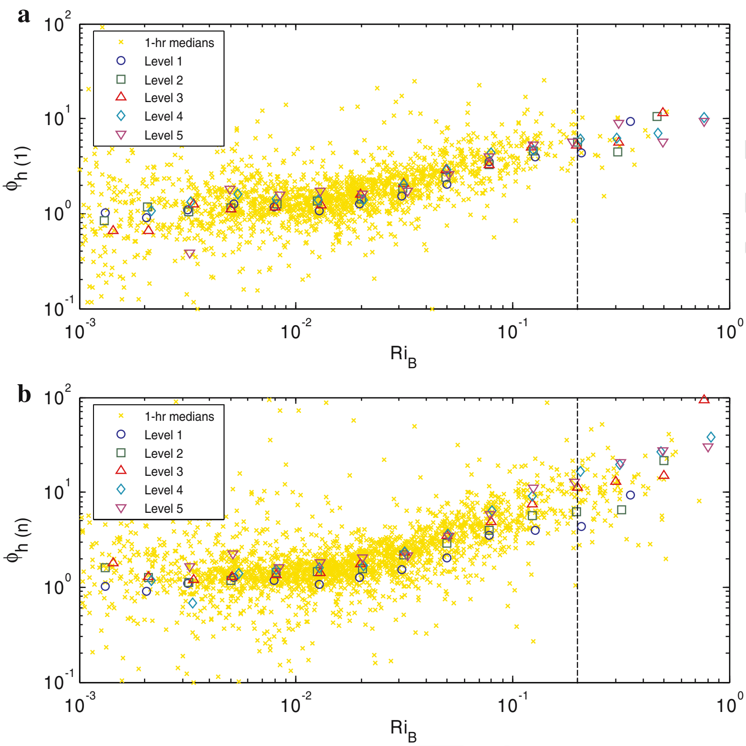

Fig. 2 Same as Fig. 1 but for the non-dimensional temperature gradient, φ_h. Data with a temperature difference between the air (at median level) and the snow surface less than 0.5°C have been omitted to avoid the large uncertainty in determining the sensible heat flux

up to $\zeta \approx 100$. Therefore, it makes sense to plot the φ_m and φ_h functions versus ζ in the range $\zeta \leq 100$.

Plots of the non-dimensional gradients of the wind speed and temperature versus the stability parameter for the five tower levels during the 11 months of the SHEBA measurements are presented in Figs. 4 and 5. These functions are plotted in the log-log coordinates for z_n/L_1 and $z_n/L_n \leq 100$ (cf. Fig. 3).

As discussed above, plots of $\varphi_m(\zeta)$ and $\varphi_h(\zeta)$ versus ζ are affected by self-correlation. For this reason, the plain bin-averaging used in Figs. 1 and 2 would be affected if used in Figs. 4 and 5, too. To reduce or even to avoid the averaging problems associated with self-correlation, in Figs. 4 and 5 we used an independent bin-averaging method instead of conventional averaging in Figs. 1 and 2. First, we sorted the data for the value of one parameter (sorting parameter) into bins. We averaged z_n/L_1 (Figs. 4a, 5a) and z_n/L_n (Figs. 4b, 5b) in bins of width $10^{0.2}$. We then computed mean and median values of $< u'w' >$, $< w'T' >$, $\mathrm{d}U/\mathrm{d}z$, $\mathrm{d}\theta/\mathrm{d}z$, and other relevant variables for each bin. Based on these averaged values, we finally computed stability parameters (1) and φ functions (2) for the surface and local scaling. Furthermore, stability parameters plotted on the horizontal axis are based on the mean values, and the φ functions plotted on the vertical axis are based on the medians.

Journal: BOUN MS: BOUN77R2 CMS: 10546_2007_9177_Article TYPESET DISK LE CP Disp.:2007/3/14 Pages:

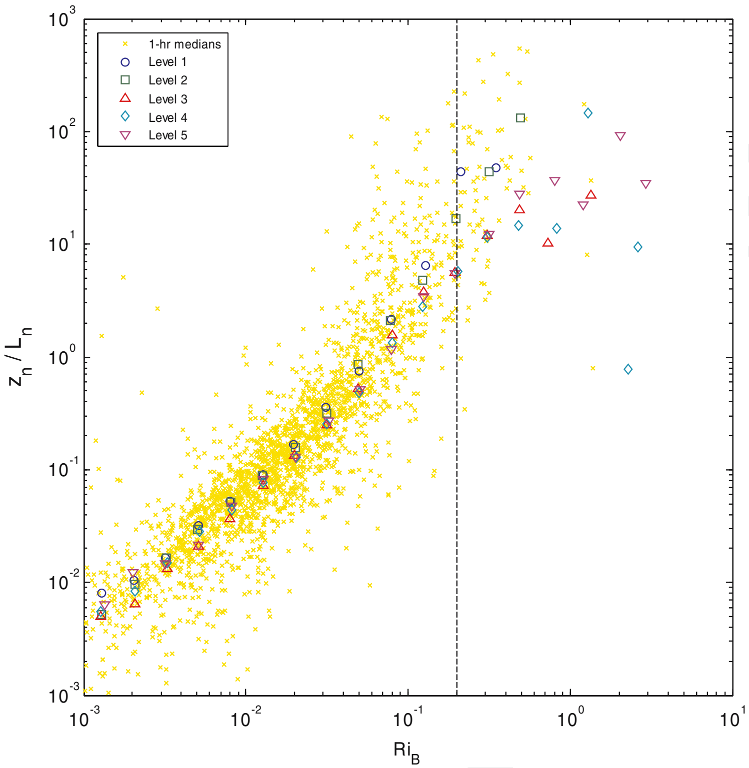

Fig. 3 Dependence of the local stability parameter, z_n/L_n, on the bulk Richardson number, Ri_B. The vertical dashed line corresponds to the critical Richardson number, $\mathrm{Ri}_B = 0.2$. Symbols are the same as in Fig. 1

According to the SHEBA data presented in Fig. 4, the stability function φ_m increases more slowly than predicted by the linear Eq. 4a and follows a $\zeta^{1/3}$ dependence in the very stable regime (cf. Grachev et al. 2005, their Fig. 14; Yagüe et al. 2006, their Figs. 3, 4). At the same time, the stability function φ_h initially increases with increasing ζ, reaches a maximum at $\zeta \approx 10$, and tends to level off at large ζ (Fig. 5). This behaviour means that the temperature profile becomes logarithmic again under very stable conditions. According to Figs. 4 and 5, using surface scaling instead of local scaling leads to less scatter between different observation levels for both φ_m and φ_h, especially for strong stability (cf. Figs. 1, 2). However, both stability functions φ_m and φ_h expressed with local scaling (Figs. 4b, 5b) show slightly better fits with the Beljaars–Holtslag relationships than those expressed with surface scaling (Figs. 4a, 5a). Cheng and Brutsaert's (2005) parameterization, based on the CASES-99 data ($\zeta \leq 5$), assumes that both functions level off for strongly stable conditions. The SHEBA data agree well with the Cheng and Brutsaert relationship for φ_m (their Eq. 22) up to $\zeta \leq 3$ but do not support their asymptotic behaviour for this function (Fig. 4a). In contrast, the Cheng and Brutsaert relationship for φ_h (their Eq. 24) describes well the asymptotic behaviour of the SHEBA data but overestimates the data in the range $0.1 \leq \zeta \leq 5$ (Fig. 5a). In addition, the variation of the turbulent Prandtl number based on the Cheng and Brutsaert parameterization with stability

Journal: BOUN MS: BOUN77R2 CMS: 10546_2007_9177_Article TYPESET DISK LE CP Disp.:2007/3/14 Pages:

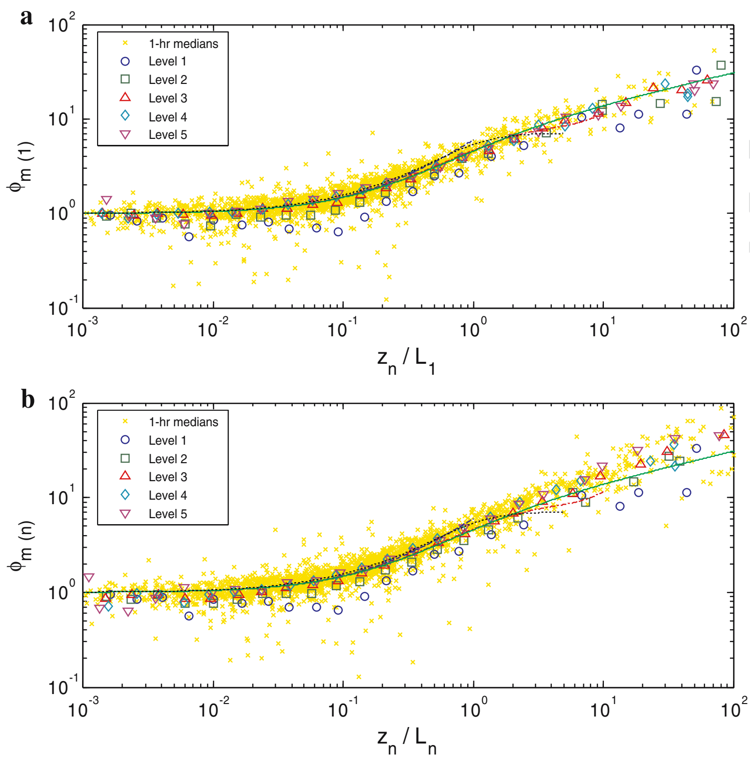

Fig. 4 Plots of the bin-averaged non-dimensional velocity gradient, φ_m, in log–log coordinates against (**a**) the surface stability parameter, z_n/L_1, and (**b**) the local stability parameter, z_n/L_n, for five levels ($n = 1 - 5$) during the 11 months of measurements. The dashed line represents $\varphi_m = \varphi_h = 1 + \beta\zeta$ with $\beta = 5(\zeta < 1)$, the dashed-dotted line is based on the Beljaars and Holtslag (1991) formula ($\zeta < 10$), and the dotted line is the Cheng and Brutsaert (2005) parameterization ($\zeta < 5$). The solid line is $\varphi_{m\ \mathrm{SHEBA}}$, Eq. 9a. Function $\varphi_{m\ (1)}$ and L_1 (upper panel) are based on the 'surface fluxes', whereas $\varphi_{m\ (n)}$ and L_n (bottom panel) are based on the 'local fluxes'. The wind speed gradient in both functions, $\varphi_{m\ (1)}$ and $\varphi_{m\ (n)}$, is based on the measurements at level n. Individual 1-h averaged data based on the median fluxes for the five levels are shown as the background x-symbols

is not monotonic in contrast to the monotonic decrease in the SHEBA data (see Sect. 5). Note, that Yagüe et al. (2006) using SABLES-98 data also reported that φ_m and φ_h tend to level off for $\zeta > 1 - 2$, whereas Hartogensis and De Bruin (2005) found good agreement between CASES-99 data and the Beljaars and Holtslag (1991) relationships.

Grachev et al. (2005) noted that the observed dependence $\varphi_m \propto \zeta^{1/3}$ (Fig. 4a) can be formally derived from Eq. 2a if one assumes that $\mathrm{d}U/\mathrm{d}z$ is independent of u_* for $\zeta >> 1$, implying that the stress (or friction velocity, u_*) is no longer a primary scaling parameter in the equation for $\mathrm{d}U/\mathrm{d}z$; they termed this regime frictionless (or 'u_*-less') scaling by analogy with the concept of 'z-less' scaling. The dramatic reduction of the surface stress is responsible for the main features of the atmospheric boundary layer in the limit of very strong stability. First, this regime is associated with the strong influence of the Earth's rotation. Frictional effects become negligible and the influence of the Coriolis effect becomes significant. Observed wind speeds show features of the

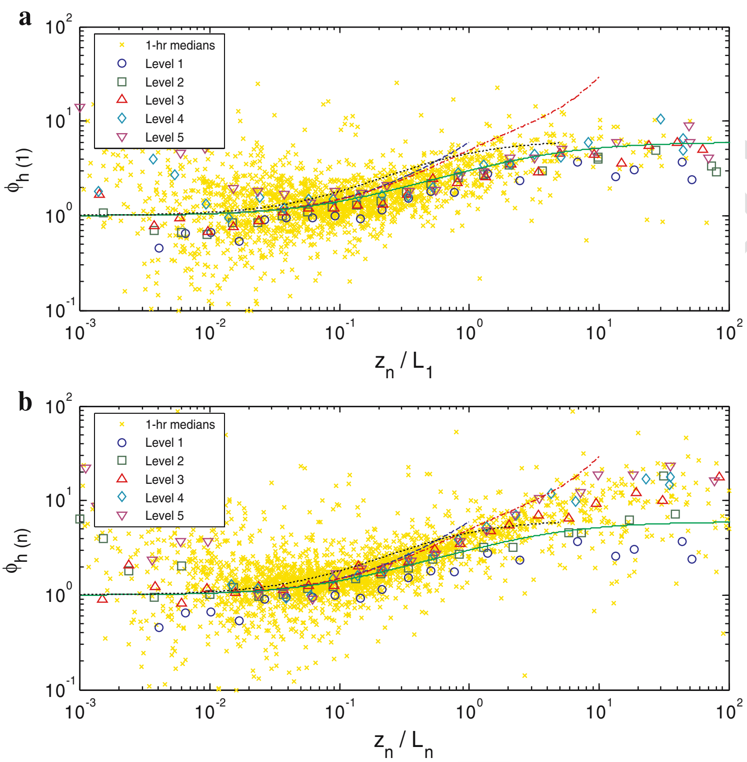

Fig. 5 Same as Fig. 4 but for the non-dimensional temperature gradient, φ_h. Data with a temperature difference between the air (at median level) and the snow surface less than 0.5°C have been omitted to avoid the large uncertainty in determining the sensible heat flux

Ekman spiral even near the surface (Grachev et al. 2002, 2005). Second, the stress falls off faster with increasing stability than the heat flux (Grachev et al. 2002, 2003, 2005), and the stress ceases to be a relevant scaling parameter in the relationship for $\mathrm{d}U/\mathrm{d}z$ in the limit of very strong stability. However, it is unlikely that the 'u_*-less' concept can be applied to φ_h. This approach would lead to the dependence $\varphi_h \propto \zeta^{-1/3}$, but according to Fig. 5, φ_h tends to be a constant in the range $10 < \zeta < 100$. According to Grachev et al. (2005, Fig. 15), some decrease in φ_h is observed for $\zeta > 100$ (cf. Yagüe et al. 2006, their Figs. 7, 8), but this is associated with the supercritical regime and may result largely from self-correlation.

According to Figs. 4 and 5, the bin averages for both φ_m and φ_h at levels 3–5 collapse better to a single curve over a wide range of z/L than the data obtained at levels 1 and 2. The data for these two lower levels are systematically lower than the data at the three higher levels. This bias is more pronounced in the wind speed profile for weakly and moderately stable conditions ($0.01 < z/L < 1$) and a possible reason of this phenomenon is discussed below. For this reason new parameterizations for φ_m and φ_h (Sect. 5) are based on the data collected at levels 3–5.

In Fig. 6, we examine the departure of the wind-speed at levels 1–5 from the logarithmic profile for near-neutral conditions ($z_n/L_n < 0.1$ and $U > 4\,\mathrm{m\,s^{-1}}$). According to Fig. 6, the wind speeds at levels 4 and 5 are more or less described by the logarith-

Journal: BOUN MS: BOUN77R2 CMS: 10546_2007_9177_Article TYPESET DISK LE CP Disp.:2007/3/14 Pages:

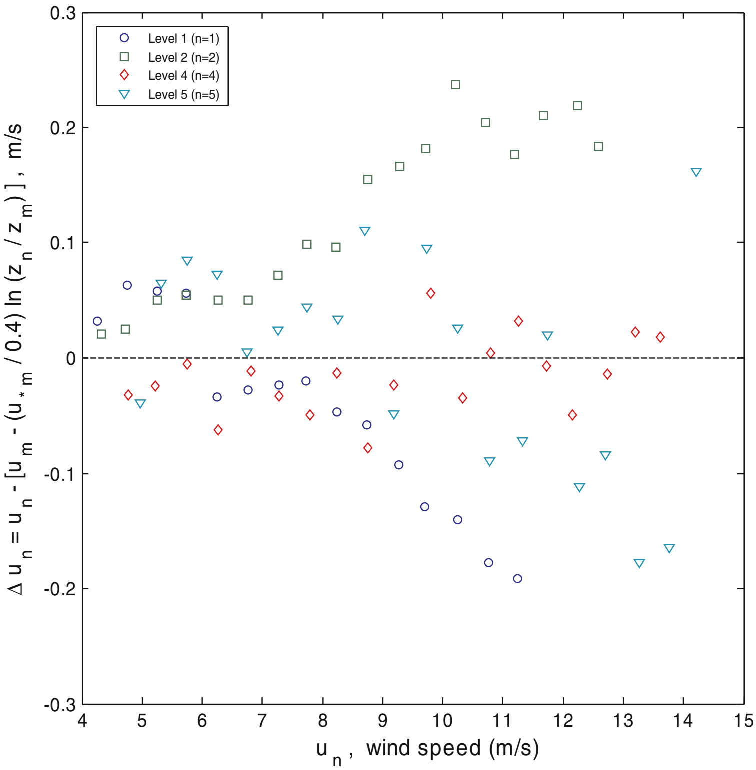

Fig. 6 Deviation of the wind speed at levels 1–5 from the logarithmic law for near-neutral conditions ($z_n/L_n < 0.1$ and $U > 4\,\mathrm{m\,s^{-1}}$). In the calculations, $u_{*\,m}$ is the median friction velocity, while u_m and z_m refer to level 3. For simplicity, stability corrections are not used here

mic law. For $U > 7 - 8\,\mathrm{m\,s^{-1}}$, the wind speed at level 1 is systematically lower and at level 2 is systematically higher than predicted by the logarithmic law. Although the deviation is small (about $0.2\,\mathrm{m\,s^{-1}}$ at $U \approx 10\,\mathrm{m\,s^{-1}}$, i.e. 2%) this behaviour may lead to the pronounced bias in the wind-speed gradients. The observed departure from the logarithmic profile in Fig. 6 may represent a real physical process, e.g. the logarithmic profile along the lower part of the tower is not in steady-state for winds higher than 7–8 $\mathrm{m\,s^{-1}}$, a surface flux footprint effect, or a blowing snow effect. It may also be a measurement artefact associated with this wind speed range. However as mentioned earlier, this effect has no impact on our parameterizations derived in this range from the measurements at levels 3–5 only.

5 The SHEBA stability functions

Traditional linear (Webb 1970; Businger et al. 1971; Dyer 1974) and Beljaars and Holtslag (1991) relationships fit most atmospheric datasets well for small and moderate values ζ when $\zeta > 0$. However, they overestimate existing data for large ζ. In essence, for large ζ, the linear relationships (4) and the Beljaars–Holtslag equation for φ_m are based on the z-less stratification concept. Although the Cheng and Brutsaert

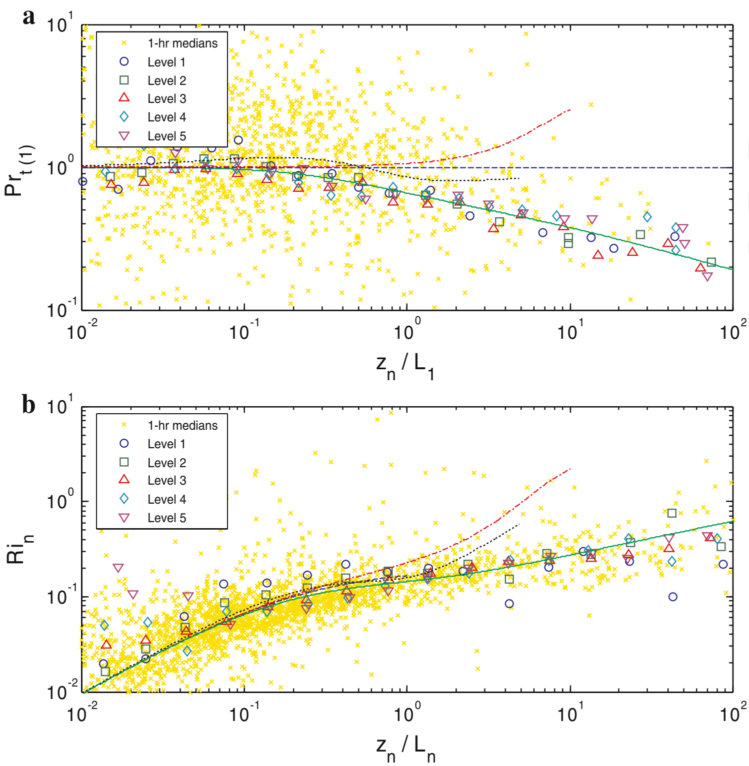

Fig. 7 Plots of the bin-averaged turbulent Prandtl number, Pr_t, (**a**) and gradient Richardson number, Ri, (**b**) versus ζ. Notation for symbols and lines is the same as in Figs. 4 and 5

(2005) parameterization is based on the recent CASES-99 data and covers a range up to $\zeta \approx 5$, there is some discrepancy between their results and the SHEBA data, as discussed above. In this section, we propose new functional forms for φ_m and φ_h in stable conditions based on the SHEBA data.

The functional forms for $\varphi_m(\zeta)$ and $\varphi_h(\zeta)$ proposed here are based on the following principals: (i) the functions should have proper behaviour, i.e., $\varphi_m(\zeta) \rightarrow 1 + \beta_m \zeta$ and $\varphi_h(\zeta) \rightarrow 1 + \beta_h \zeta$ for small ζ, and $\varphi_m \propto \zeta^{1/3}$ and $\varphi_h \rightarrow$ constant for $\zeta \rightarrow \infty$; (ii) $\varphi_m(\zeta)$ and $\varphi_h(\zeta)$ should fit the SHEBA data reasonably well for the entire range of $\zeta > 0$; and (iii) $\varphi_m(\zeta)$ and $\varphi_h(\zeta)$ should be analytically integrable, that is, $\Psi_m(\zeta)$ and $\Psi_h(\zeta)$ should be analytical functions (see Eq. 6).

A number of functions that satisfy the above criteria have been tested. Note that some interpolations suggested earlier for free convection and modified for $\zeta > 0$ can be applied here for $\varphi_m(\zeta)$. Power law interpolations have the general form suggested by Wilson (2001), $\varphi_m(\zeta) = (1 + \gamma_m \zeta^{k_m})^{n_m}$ and $\varphi_h(\zeta) = (1 + \gamma_h \zeta^{k_h})^{n_h}$, while the exponent combination used by Carl et al. (1973) is $(k_m, n_m) = (k_h, n_h) = (1, -1/3)$. Kansas-type relationships are associated with the combination $(k_m, n_m) = (1, -1/4)$ and $(k_h, n_h) = (1, -1/2)$ for unstable conditions and $(k_m, n_m) = (k_h, n_h) = (1, 1)$ for stable stratification (see Eq. 4), and Wilson (2001) suggested an alternative function $(k_m, n_m) = (k_h, n_h) = (2/3, -1/2)$ for $\zeta < 0$. These functions, however, have the undesirable property that the derivatives of both φ_m and φ_h approach infinity as ζ approaches zero.

The concept of 'u_*-less' stratification requires that $k_m n_m = 1/3$. The following combinations have been tested on the SHEBA dataset (k_m , n_m) = (1/3, 1), (1, 1/3), (2/3, 1/2), (1/2, 2/3). Our analysis demonstrated that all these cases lead to unsatisfactory agreement with the data. Thus, a simple interpolation with one coefficient (γ_m) cannot describe the SHEBA data. Functional forms suggested by Kader and Yaglom (1990, their Eq. 3.6) for $\zeta < 0$ with several calibration coefficients could also be adopted for the stable case, but these equations are not analytically integrable.

We thus suggest the following functional forms of $\varphi_m(\zeta)$ and $\varphi_h(\zeta)$ based on the SHEBA data ('the SHEBA profile functions'):

$$\varphi_{m\ \mathrm{SHEBA}} = 1 + \frac{a_m \zeta (1+\zeta)^{1/3}}{1 + b_m \zeta} \equiv 1 + \frac{6.5\zeta(1+\zeta)^{1/3}}{1.3+\zeta}, \tag{9a}$$

$$\varphi_{h\ \mathrm{SHEBA}} = 1 + \frac{a_h \zeta + b_h \zeta^2}{1 + c_h \zeta + \zeta^2} \equiv 1 + \frac{5\zeta + 5\zeta^2}{1 + 3\zeta + \zeta^2}, \tag{9b}$$

where $a_m \equiv \beta_m = 5$, $b_m = a_m/6.5$, $a_h \equiv \beta_h = 5$, $b_h = 5$, and $c_h = 3$. Coefficients a_m and a_h are determined from the asymptotic behaviour of $\varphi_m(\zeta)$ and $\varphi_h(\zeta)$ for small ζ (see Eq. 4); the ratio a_m/b_m and coefficient b_h are derived from the asymptotic behaviour of these functions at $\zeta \to \infty$. Note that $\varphi_m \to (a_m/b_m)\zeta^{1/3} = 6.5\zeta^{1/3}$ and $\varphi_h \to 1 + b_h = 6$ as $\zeta \to \infty$. Coefficient c_h is derived by fitting the data for moderate ranges of ζ. The proposed parameterizations for the stability functions φ_m and φ_h, Eq. 9, are plotted versus the stability parameter in Figs. 4 and 5 (solid lines). As discussed above, the surface scaling is superior to the local scaling.

Parameterizations (9) have also been used to study the behaviour of the turbulent Prandtl number and the gradient Richardson number (Fig. 7) (cf. Andreas 2002). Note that the difference between φ_m and φ_h is best demonstrated by plots of the turbulent Prandtl number defined by

$$\mathrm{Pr}_t = \frac{k_m}{k_h} = \frac{< u'w' > \ \mathrm{d}\theta/\mathrm{d}z}{< w'\theta' > \mathrm{d}U/\mathrm{d}z} \equiv \frac{\varphi_h}{\varphi_m}, \tag{10}$$

where $k_m = -\frac{<u'w'>}{\mathrm{d}U/\mathrm{d}z}$ is the turbulent viscosity, and $k_h = -\frac{<w'\theta'>}{\mathrm{d}\theta/\mathrm{d}z}$ is the turbulent thermal diffusivity. The turbulent Prandtl number (10) describes the difference in turbulent transfer between momentum and sensible heat; turbulent momentum transfer is more efficient than turbulent heat transfer when $\mathrm{Pr}_t > 1$ and vice versa.

The gradient Richardson number, Ri, is defined by

$$\mathrm{Ri} = \left(\frac{g}{\theta_v}\right) \frac{\mathrm{d}\theta_v/\mathrm{d}z}{(\mathrm{d}U/\mathrm{d}z)^2} = \frac{\zeta \varphi_h}{\varphi_m^2}. \tag{11}$$

Note that Pr_t and Ri depend more sensitively on the parameterizations for $\varphi_m(\zeta)$ and $\varphi_h(\zeta)$ because both parameters numbers are combinations of φ_m and φ_h. The flux Richardson number, in contrast, contains only one function, $\mathrm{Rf} = \zeta/\varphi_m$. According to Eq. 10, Pr_t may be defined for local and for surface scaling as we have done for $\varphi_m(\zeta)$ and $\varphi_h(\zeta)$. The relationship (11) for Ri contains no fluxes, and therefore Ri is defined only locally.

According to Fig. 7a, on average, Pr_t tends to be less than 1 with increasing stability by virtue of the asymmetric behaviour of the φ_m and φ_h functions (Figs. 1, 2, 4 and 5).

Journal: BOUN MS: BOUN77R2 CMS: 10546_2007_9177_Article TYPESET DISK LE CP Disp.:2007/3/14 Pages:

Note also that according to Grachev et al. (2002, 2003, 2005), a small but still significant heat flux (several $\mathrm{w\,m^{-2}}$) and negligibly small stress characterize the very stable regime. This asymmetric flux decay causes k_m to decrease faster than k_h and therefore leads Pr_t to decrease (see Eq. 10). Our result $\mathrm{Pr}_t < 1$ is consistent with Howell and Sun (1999) but disagrees with the measurements of Kondo et al. (1978) and Yagüe et al. (2001), the Beljaars and Holtslag (1991) relation, and the Zilitinkevich and Calanca (2000) model.

Note also that a plot of Ri versus ζ by definition is not affected by the self-correlation. For this reason, Fig. 7b is simply a plot of Ri versus z_n/L_n. The plots in Fig. 7 are an additional verification of the proposed SHEBA profile functions (9) (solid lines in the figure). The greater scatter of points in Fig. 7 for $\zeta < 0.05$ results from the relatively small sensible heat flux and unreliable temperature-gradient measurements in near-neutral conditions. The obtained asymptotic behaviours of $\varphi_m(\zeta)$ and $\varphi_h(\zeta)$ for $\zeta \to \infty$ imply that $\mathrm{Pr}_t \propto \zeta^{-1/3}$, $\mathrm{Ri} \propto \zeta^{1/3}$, and $\mathrm{Rf} \propto \zeta^{2/3}$ in the limit of very strong stability.

The integral form of $\varphi_{m\ \mathrm{SHEBA}}$ can be obtained by integrating Eq. 6a with $\varphi_m(\zeta)$ defined by Eq. 9a,

$$\Psi_{m\ \mathrm{SHEBA}}(\zeta) = \int_0^\zeta \frac{1-\varphi_{m\ \mathrm{SHEBA}}(\xi)}{\xi}\mathrm{d}\xi$$
$$= -\frac{3a_m}{b_m}(x-1) + \frac{a_m B_m}{2b_m}\left[2\ln\frac{x+B_m}{1+B_m} - \ln\frac{x^2 - xB_m + B_m^2}{1 - B_m + B_m^2}\right.$$
$$\left. +2\sqrt{3}\left(\arctan\frac{2x-B_m}{\sqrt{3}B_m} - \arctan\frac{2-B_m}{\sqrt{3}B_m}\right)\right], \qquad (12)$$

where $x = (1+\zeta)^{1/3}$, $B_m = \left(\frac{1-b_m}{b_m}\right)^{1/3} > 0$. In a similar way to Eq. 12, the integral form of the $\varphi_{h\ \mathrm{SHEBA}}$ can be obtained from Eqs. 6b, 9b:

$$\Psi_{h\ \mathrm{SHEBA}}(\zeta) = \int_0^\zeta \frac{1-\varphi_{h\ \mathrm{SHEBA}}(\xi)}{\xi}\mathrm{d}\xi$$
$$= -\frac{b_h}{2}\ln\left(1 + c_h\zeta + \zeta^2\right) + \left(-\frac{a_h}{B_h} + \frac{b_h c_h}{2B_h}\right)$$
$$\times\left(\ln\frac{2\zeta + c_h - B_h}{2\zeta + c_h + B_h} - \ln\frac{c_h - B_h}{c_h + B_h}\right), \qquad (13)$$

where $B_h = \sqrt{c_h^2 - 4} = \sqrt{5}$. Equations 12 and 13 are more complicated than the Kansas-type, the Beljaars–Holtslag, and Cheng–Brutsaert $\Psi_m(\zeta)$ and $\Psi_h(\zeta)$functions. However, Eqs. 12 and 13 are analytical relationships based on the $\varphi_m(\zeta)$ and $\varphi_h(\zeta)$ functions (9a) and (9b) that better fit the SHEBA data. Applying the functional forms (12) and (13) to wind speed (5a) and temperature (5b) profiles is straightforward. The proposed SHEBA profile functions (9) are valid for $\mathrm{Ri}_B < \mathrm{Ri}_{B\,cr} \approx 0.2$. The bulk Richardson number, Eq. 8, may be estimated from Eqs. 5, 12, and 13.

6 Conclusions

We have used the comprehensive SHEBA flux–profile data to understand the behaviour of the profile stability functions, φ_m and φ_h, and derive quantities such

Journal: BOUN MS: BOUN77R2 CMS: 10546_2007_9177_Article TYPESET DISK LE CP Disp.:2007/3/14 Pages:

as the turbulent Prandtl number, Pr_t, and the gradient Richardson number in the stably stratified atmospheric boundary layer.

According to the SHEBA data, both stability functions φ_m and φ_h increase more slowly in very stable conditions than predicted by the linear equations (4) and the Beljaars–Holtslag relationship. In the limit of very strong stability, φ_m varies as $\zeta^{1/3}$; whereas φ_h initially increases with increasing ζ, reaches a maximum at $\zeta \approx 10$, and then tends to level off with increasing ζ. The scaling law $\varphi_m \propto \zeta^{1/3}$ is associated with our proposed frictionless or 'u_*-less' scaling. As a consequence of the observed dependences for the stability functions φ_m and φ_h, the turbulent Prandtl number decreases and tends to be less than 1 ($Pr_t \propto \zeta^{-1/3}$) with increasing stability. This result implies that heat transfer is more efficient than momentum transfer in the very stable regime.

Based on the SHEBA data, we propose new mathematical forms for φ_m and φ_h in stable conditions, Eq. 9. The SHEBA measurements also show that profile stability functions based on local scaling are more scattered than those based on surface scaling. We took special care when analyzing φ_m and φ_h as functions of ζ in light of the self-correlation problem. For independent estimates of how φ_m and φ_h behave in very stable stratification, we plotted these functions against the bulk Richardson number. In addition, to analyze φ_m and φ_h as functions of ζ, we used an independent bin-averaging method instead of conventional averaging.

Acknowledgements The U.S. National Science Foundation supported this work with awards to the NOAA Environmental Technology Laboratory (now Earth System Research Laboratory) (OPP-97-01766), the Cooperative Institute for Research in Environmental Sciences (CIRES), University of Colorado (OPP-00-84322, OPP-00-84323), the U.S. Army Cold Regions Research and Engineering Laboratory (OPP-97-02025, OPP-00-84190), and the Naval Postgraduate School (OPP-97-01390, OPP-00-84279). The U.S. Department of the Army also supported ELA through Project 611102T2400. Thanks go to Reg Hill and Bob Banta for suggestions on improving the manuscript. Comments from anonymous reviewers are greatly appreciated.

References

Andreas EL (2002) Parameterizing scalar transfer over snow and ice: a review. J Hydrometeorol 3:417–432

Andreas EL, Hicks BB (2002) Comments on critical test of the validity of Monin-Obukhov similarity during convective conditions. J Atmos Sci 59:2605–2607

Andreas EL, Fairall CW, Guest PS, Persson POG (1999) An overview of the SHEBA atmospheric surface flux program. 13th symposium on boundary layers and turbulence. Dallas, TX, Amer Meteorol Soc, Proceedings, pp 550–555

Andreas EL, Claffey KJ, Makshtas AP (2000) Low-level atmospheric jets and inversions over the Western Weddell Sea. Boundary-Layer Meteorol 97:459–486

Andreas EL, Claffey KJ, Jordan RE, Fairall CW, Guest PS, Persson POG, Grachev AA (2006) Evaluations of the von Kármán constant in the atmospheric surface layer. J Fluid Mech 559: 117–149

Andreas EL, Guest PS, Persson POG, Fairall CW, Horst TW, Moritz RE, Semmer SR (2002) Near-surface water vapor over sea ice is always near ice saturation. J Geophys Res 107(C10), doi: 10.1029/2000JC000411

Andreas EL, Fairall CW, Grachev AA, Guest PS, Horst TW, Jordan RE, Persson POG (2003) Turbulent transfer coefficients and roughness lengths over sea ice: the SHEBA results. In Seventh conference on polar meteorology and oceanography and joint symposium on high-latitude climate variations, American Meteorological Society. 12–16 May 2003, Hyannis, Massachusetts, AMS Preprint CD-ROM (http://ams.confex.com/ams/7POLAR/7POLARCLIM/abstracts/60666.htm)

Beljaars ACM, Holtslag AAM (1991) Flux parameterization over land surfaces for atmospheric models. J Appl Meteorol 30(3):327–341

Businger JA, Wyngaard JC, Izumi Y, Bradley EF (1971) Flux–profile relationships in the atmospheric surface layer. J Atmos Sci 28:181–189

Carl MD, Tarbell TC, Panofsky HA (1973) Profiles of wind and temperature from towers over homogeneous terrain. J Atmos Sci 30:788–794

Cheng Y, Brutsaert W (2005) Flux–profile relationships for wind speed and temperature in the stable atmospheric boundary layer. Boundary-Layer Meteorol 114(3):519–538

Clement RJ (2004) Mass and energy exchange of a plantation forest in Scotland using micrometeorological methods. PhD Thesis, The University of Edinburgh, School of Geosciences, 597 p. (http://www.geos.ed.ac.uk/homes/rclement/PHD/)

Dyer AJ (1974) A review of flux–profile relationships. Boundary-Layer Meteorol. 7:363–372

Dyer AJ, Bradley EF (1982) An alternative analysis of flux–gradient relationships at the 1976 ITCE. Boundary-Layer Meteorol 22:3–19

Dyer AJ, Hicks BB (1970) Flux–gradient relationships in the constant flux layer. Quart J Roy Meteorol Soc 96:715–721

Forrer J, Rotach MW (1997) On the turbulence structure in the stable boundary layer over the greenland ice sheet. Boundary-Layer Meteorol 85:111–136

Garratt JR (1992) The atmospheric boundary layer. Cambridge University Press, Cambridge, 316 pp

Grachev AA, Fairall CW, Persson POG, Andreas EL, Guest PS (2002) Stable boundary-layer regimes observed during the SHEBA Experiment. In 15th symposium on boundary layers and turbulence. Wageningen, The Netherlands, Amer. Meteorol. Soc., Proc., 374 – 377 (PDF file: http://ams.confex.com/ams/BLT/15BLT/abstracts/43715.htm)

Grachev AA, Fairall CW, Persson POG, Andreas EL, Guest PS, Jordan RE (2003) Turbulence decay in the stable arctic boundary layer.In Seventh conference on polar meteorology and oceanography and joint symposium on high-latitude climate variations. Hyannis, Massachusetts, Amer. Meteorol. Soc., Preprint CD-ROM (PDF file: http://ams.confex.com/ams/7POLAR/7POLARCLIM/abstracts/61456.htm)

Grachev AA, Fairall CW, Persson POG, Andreas EL, Guest PS (2005) Stable boundary-layer scaling regimes: The SHEBA data. Boundary-Layer Meteorol 116(2):201–235

Hartogensis OK, De Bruin HAR (2005) Monin–Obukhov similarity functions of the structure parameter of temperature and turbulent kinetic energy dissipation rate in the stable boundary layer. Boundary-Layer Meteorol 116(2):253–276

Hicks BB (1978) Comments on 'The characteristics of turbulent velocity components in the surface layer under convective conditions'. by H. A. Panofsky, et al. Boundary-Layer Meteorol. 15(2):255–258

Högström U (1988) Non-dimensional wind and temperature profiles in the atmospheric surface layer: a re-evaluation. Boundary-Layer Meteorol 42:55–78

Holtslag AAM, De Bruin HAR (1988) Applied modeling of the nighttime surface energy balance over land. J Appl Meteorol 27:689–704

Holtslag AAM, Nieuwstadt FTM (1986) Scaling the atmospheric boundary layer. Boundary-Layer Meteorol 36:201–209

Horst T (2000) On frequency response corrections for eddy covariance flux measurements. Boundary-Layer Meteorol 94(3):517–520

Howell JF, Sun J (1999) Surface-layer fluxes in stable conditions. Boundary-Layer Meteorol 90:495–520

Kader BA, Yaglom AM (1990) Mean fields and fluctuation moments in unstably stratified turbulent boundary layers. J Fluid Mech 212:637–662

Kaimal JC, Finnigan JJ (1994) Atmospheric boundary layer flows: their structure and measurements. Oxford University Press, New York, Oxford, 289 pp

King JC (1990) Some measurements of turbulence over an antarctic shelf. Quart J Roy Meteorol Soc 116:379–400

Klipp CL, Mahrt L (2004) Flux–gradient relationship, self-correlation and intermittency in the stable boundary layer. Quart J Roy Meteorol Soc 130(601):2087–2103

Kondo J, Kanechika O, Yasuda N (1978) Heat and momentum transfers under strong stability in the atmospheric surface layer. J Atmos Sci 35:1012–1021

Kristensen L, Fitzjarrald DR (1984) The effect of line averaging on scalar flux measurements with a sonic anemometer near the surface. J Atmos Oceanic Technol 1(3):138–146

Mahrt L (1999) Stratified atmospheric boundary layers. Boundary-Layer Meteorol 90:375–396

Mahrt L, Vickers D (2002) Contrasting vertical structures of nocturnal boundary layers. Boundary-Layer Meteorol 105:351–363

Journal: BOUN MS: BOUN77R2 CMS: 10546_2007_9177_Article TYPESET DISK LE CP Disp.:2007/3/14 Pages:

Mahrt L, Sun J, Blumen W, Delany T, Oncley S (1998) Nocturnal boundary-layer regimes. Boundary-Layer Meteorol 88:255–278

Massman WJ (2000) A simple method for estimating frequency response corrections for eddy covariance systems. Agric Forest Meteorol 104:185–198

Monin AS, Obukhov AM (1954) Basic laws of turbulent mixing in the surface layer of the atmosphere. Trudy Geofiz Inst Acad Nauk SSSR 24:163–187

Monin AS, Yaglom AM (1971) Statistical fluid mechanics: mechanics of turbulence, vol 1. MIT Press, Cambridge, Massachusetts, 769 pp

Moore CJ (1986) Frequency response corrections for eddy correlation systems. Boundary-Layer Meteorol 37(1–2):17–36

Nieuwstadt FTM (1984) The turbulent structure of the stable, nocturnal boundary layer. J Atmos Sci 41:2202–2216

Obukhov AM (1946) Turbulence in an atmosphere with a non-uniform temperature. Trudy Inst Teoret Geofiz Akad Nauk SSSR 1:95–115

Obukhov AM (1971) Turbulence in an atmosphere with a non-uniform temperature. Boundary-Layer Meteorol 2:2–29

Panofsky HA (1963) Determination of stress from wind and temperature measurements. Quart J Roy Meteorol Soc 89:85–94

Pahlow M, Parlange MB, Porté-Agel F (2001) On Monin–Obukhov similarity in the stable atmospheric boundary layer. Boundary-Layer Meteorol. 99:225–248

Paulson CA (1970) The mathematical representation of wind speed and temperature profiles in the unstable atmospheric surface layer. J Appl Meteorol 9:857–861

Paw UKT, Baldocchi DD, Meyers TP, Wilson KB (2000) Correction of eddy-covariance measurements incorporating both advective effects and density fluxes. Boundary-Layer Meteorol 97(3):487–511

Persson POG, Fairall CW, Andreas EL, Guest PS, Perovich DK (2002) Measurements near the atmospheric surface flux group Tower at SHEBA: near-surface conditions and surface energy budget. J Geophys Res 107(C10):8045, doi: 10.1029/2000JC000705

Smedman A-S (1988) Observations of a multi-level turbulence structure in a very stable atmospheric boundary layer. Boundary-Layer Meteorol 44:231–253

Sorbjan Z (1989) Structure of the atmospheric boundary layer. Prentice-Hall, New Jersey, 317 pp

Uttal T, 27 co-authors (2002) Surface heat budget of the Arctic ocean. Bull Am Meteorol Soc 83:255–276

Webb EK (1970) Profile relationships: the log-linear range, and extension to strong stability. Quart J Roy Meteorol Soc 96:67–90

Wilczak JM, Oncley SP, Stage SA (2001) Sonic anemometer Tilt correction algorithms. Boundary-Layer Meteorol 99(1):127–150

Wilson DK (2001) An alternative function for the wind and temperature gradients in unstable surface layers. Boundary-Layer Meteorol 99:151–158

Wyngaard JC (1973) On surface-layer turbulence. In Haugen DA (ed) Workshop on micrometeorology. American Meteorology Society, Boston, Mass, pp 101–149

Wyngaard JC, Coté OR (1972) Cospectral similarity in the atmospheric surface layer. Quart J Roy Meteorol Soc 98:590–603

Yaglom AM (1977) Comments on wind and temperature flux–profile relationships. Boundary-Layer Meteorol 11:89–102

Yagüe C, Maqueda G, Rees JM (2001) Characteristics of turbulence in the lower atmosphere at Halley IV Station, Antarctica. Dyn Atmos Ocean 34:205–223

Yagüe C, Viana S, Maqueda G, Redondo JM (2006) Influence of stability on the flux–profile relationships for wind speed, φ_m, and temperature, φ_h, for the stable atmospheric boundary layer. Nonlin Processes Geophys 13(2):185–203

Zilitinkevich S, Baklanov A (2002) Calculation of the height of the stable boundary layer in practical applications. Boundary-Layer Meteorol 105:389–409

Zilitinkevich S, Calanca P (2000) An extended similarity-theory for the stably stratified atmospheric surface layer. Quart J Roy Meteorol Soc 126:1913–1923

Zilitinkevich SS, Chalikov DV (1968) Determining the universal wind-velocity and temperature profiles in the atmospheric boundary layer. Izvestiya Acad Sci USSR Atmos Oceanic Phys 4:165–170 (English Edition)

Zilitinkevich S, Mironov DV (1996) A multi-limit formulation for the equilibrium depth of a stably stratified boundary layer. Boundary-Layer Meteorol 81:325–351

Journal: BOUN MS: BOUN77R2 CMS: 10546_2007_9177_Article TYPESET DISK LE CP Disp.:2007/3/14 Pages: